I J C T A, 9(32), 2016, pp. 101-109 ISSN: 0974-5572

Performance Characteristics of Hybrid Pole self bearing Switched Reluctance Motor

R.S.R. Krishnam Naidu and G.V. Nagesh Kumar*

ABSTRACT

This paper presents, the performance characteristics of self-bearing hybrid pole switched reluctance motor (SBSRM). The SBSRM has two separated and independent stator pole windings for torque generation and axial force generation. The performance characteristics shows, torque and axial force are completely decoupled and also radial force exhibits excellent linear characteristics with respect to rotor position. Number of stator poles utilized for torque production are high than axial force generation poles, hence the torque output has been improved significantly. Static characteristics have been carried out using finite element method (FEM). Finally, simulation results have been presented using MATLAB environment.

Keywords: Self bearing switched reluctance motor, finite element method, conventional PID controller, MATLAB/ Simulink

1. INTRODUCTION

Present all industrial looking for high speed applications such as compressor and aerospace especially these two areas requires ultra-high speed and also fail-safe machines [1], but the conventional bearings at higher speeds causes frictional drag, lubrication oil cannot be used in ultra high speed applications [2-3]. Self bearing switched reluctance motor (SBSRM) is the combination of conventional switched reluctance motor and active magnetic bearing hence this type of motors persists the advantages of both SRM and active magnetic bearing such it can operate in very high temperature atmosphere due to no winding on rotor, it can catch ultra high speeds due to absence of bearings. [4-6]. numerous verity structures of self bearing SRM's have been existed in literature. But each structure has its own disadvantages like, reverse toque, using high converter switches, low power density, can't be utilized full torque region, critical speed is reduced in Morrison type motor, long magnetic flux paths and reversal of flux in stator core and core losses etc. to overcome the aforementioned problems with the different bearing less structures, 12/14 hybrid pole type SBSRM is presented with two types of stator poles. SBSRM has eight torque pole (A_1 to A_4 which are in series connection to form A-Phase winding and B_1 to B_4 which are in series connection to form B-Phase winding as shown in fig.1), 4 radial force poles (P_{s1}, P_{s2}, P_{s3} and P_{s4}) on stator and 14 poles on rotor. Characteristics show that radial force is completely decoupled from torque.

Section-I presents the introduction and literature survey on bearing less motors and also presented the need to go for 12/14 self bearing switched reluctance motor and its stator and rotor pole information. Section-II presents the mechanical design and controlling scheme of 12/14 SBSRM. Section-III presents the description of performance characteristics and also shows the magnetic flux distribution of 12/14 self bearing hybrid pole switched reluctance motor. Section IV presents the simulation block diagram and results.

[1] GITAM Institute of Technology, GITAM University Visakhapatnam, India.

* Corresponding Author: gundavarapu_kumar@yahoo.com

2. 12/14 SELF BEARING SWITCHED RELUCTANCE MOTOR

A 12/14 SBSRM is described in this section and its structure is shown in Fig.1. SBSRM has eight torque pole (A_1 to A_4 which are in series connection to form A-Phase winding and B_1 to B_4 which are in series connection to form B-Phase winding as shown in fig.1), 4 radial force poles (P_{s1}, P_{s2}, P_{s3} and P_{s4}) on stator, 4 radial force poles (P_{s1}, P_{s2}, P_{s3} and P_{s4}), are independently connected in x and y directions and 14 poles on rotor. The generated torque shows the independent nature with the generated radial force, hence torque and suspension forces can be controlled independently. As shown in this figure, this motor used higher portion of stator poles for generating torque, hence improve power density, and decrease the requirement of magneto motive force (MMF) and also decrease the iron and cupper losses (core losses). Fig.2. shows the Prototype of SBSRM. Table-I shows the dimensions of the SBSRM. Fig.3 depicts the real time hardware control

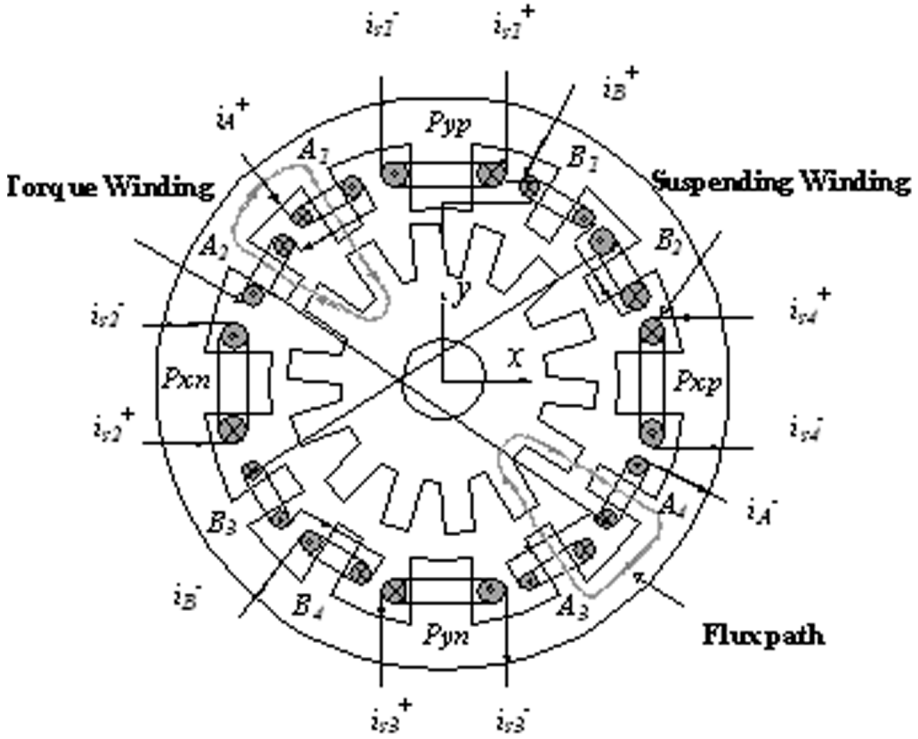

Figure 1: Structure of SBSRM

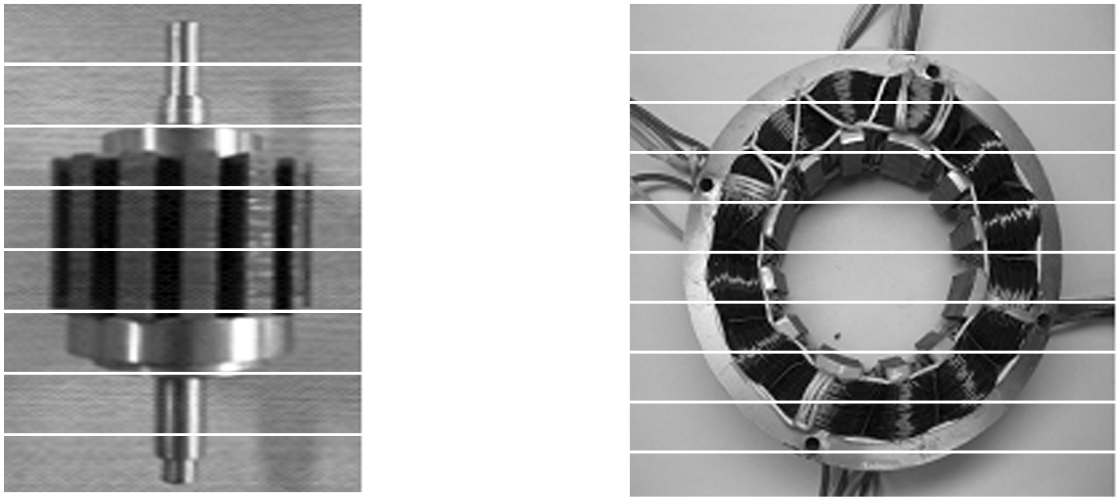

(a) Rotor **(b) Stator**

Figure 2: Prototype of SBSRM

mechanism of both torque and axial force controlling of the SBSRM. X* and Y* are the commend displacement signals, the values of command displacements are zero, it means that rotor is being in center position. These command displacement signals have been compared with the signals which are coming from two displacement sensors, one is placed in X-direction and another one is placed in Y direction. The sensitivity of the displacement sensors is 5V/mm. the error signals are given to the conventional PID controller. The output of the PID controllers are Fx* and Fy*, these are the command forces need to bring the rotor to center position. These command forces are converted into command currents and compared with suspension currents. The error current signals are given to the PWM logic block and generate PWM

Table 1
Dimensions SBSRM

	Parameter	*SBSRM*
stator poles		12
rotor poles		14
	Stator torque pole	12.85 (deg)
Arc angle	Stator axial pole	25.7 (deg)
	Rotor pole	12.85 (deg)
Length	Axial stack	40(mm)
	Air gap	0.3(mm)
Diameter	Outer stator	112 (mm)
	Inner stator	60.2 (mm)
Yoke thickness of rotor (mm)		7.7(mm)
No. of winding turns per pole	Torque	80
	Axial force	100

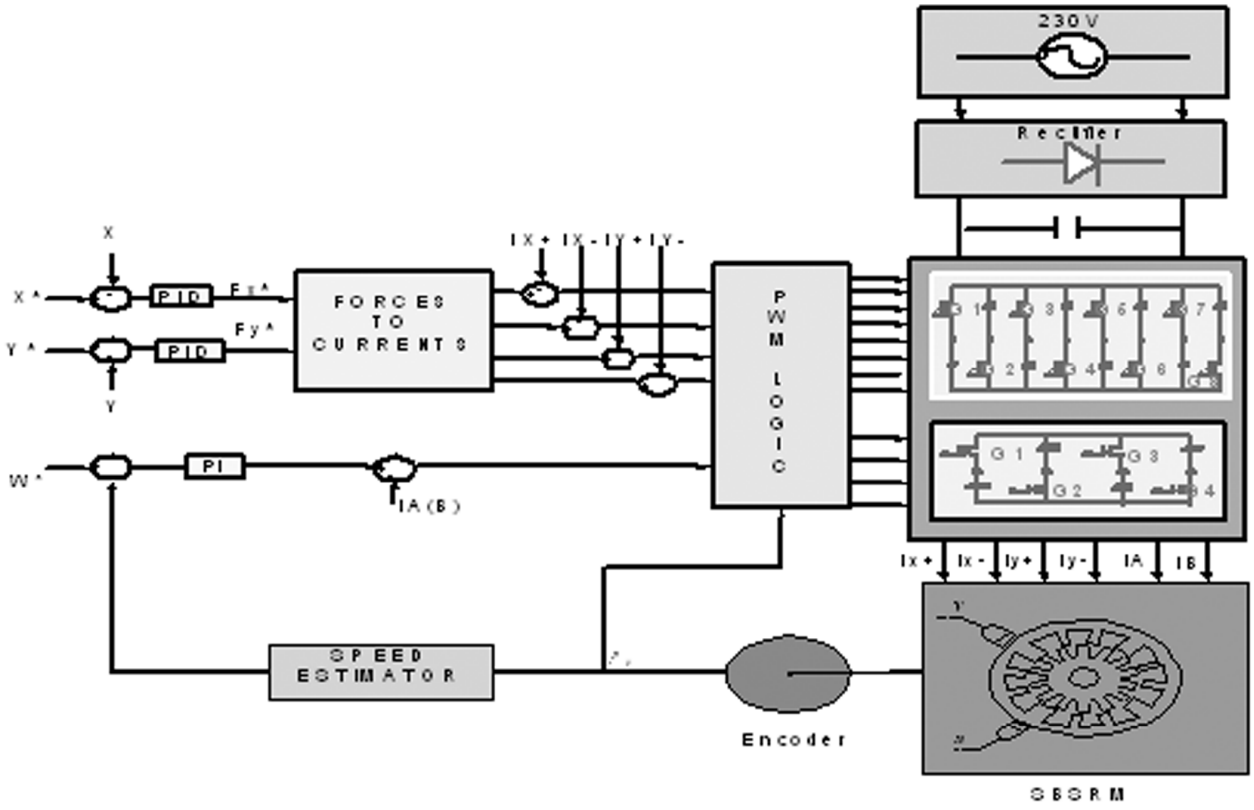

Figure 3: Control scheme of SBSRM

signals to the 4- phase asymmetric converter. This 4-phase converter suspends the rotor to the center position according the generated PWM signals. Now encoder giving the position information of the rotor, from this position speed is calculated using speed estimator block and this speed is compared with the speed command W* (reference speed). The error speed is given to the PI controller and generates command current im* and is compare with the motor torque currents (IA and IB) and this signal is given to the PWM block to generate the PWM signals to 2-phase asymmetric converter. This 2-phase converter drives the rotor according to the generated PWM signals.

3. CHARACTERISTIC ANALYSIS OF SBSRM

The characteristics of SBSRM like flux distribution, inductance and axial force and torque have been presented.

3.1. Flux Distribution

Fig. 4 shows magnetic flux distributions of the 12/14 SBSRM. Magnetic flux paths clears that, there is no reversal of flux and also shows the short flux paths when compared to the previous motor structure of 8/10 self bearing switched reluctance motor. As a result the stator of SBSRM requires less magneto motive force (MMF), consequently has less core losses in the system. One thing can be noticed from fig. 4. is that both torque pole wining and suspension pole windings are continuously excited at every instant.

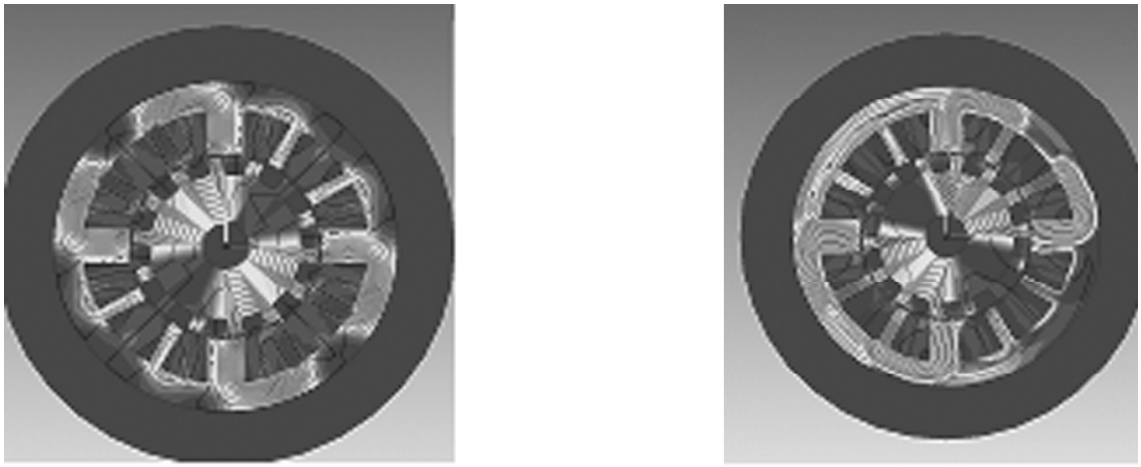

(a) Phase-A with suspending pole **(b) Phase-B with suspending pole**

Figure 4: Flux distribution in torque and radial force windings of SBSRM

3.2. Inductance

The inductance of SBSRM changes with change in rotor position as similar to conventional SRM, which is mainly due to the overlap angle between rotor pole teeth and toque pole teeth involves in the function of rotor position. Torque winding offers large inductance due to the presence of different turns of torque winding and toque poles arc. Inductance of radial force winding exhibits little change with respect to the rotor position, as the radial pole pitch is larger than the rotor pole pitch. As increases the currents in both the torque and radial force windings, it is observed that maximum inductance is decreases; this is due to the effect of core saturation. Here one thing can be noticed that core saturation is not that much when only one wining have been conducted, hence in SBSRM both the windings always been conducting for effective suspension along with rotation as shown in fig. 4(a) and 4(b).

$$L = \frac{\mu_0 N^2 L\, r}{g}\left(\theta_a + K_f\right) \tag{1}$$

Where,

μ_0 = Permeability of the free space,

N = Number of winding turns,

L = Stack length of the SBSRM,

r = Rotor Radius,

g = air gap Length,

K_f = fringing constant of inductance,

θ_a and θ_u = aligned and unaligned angle.

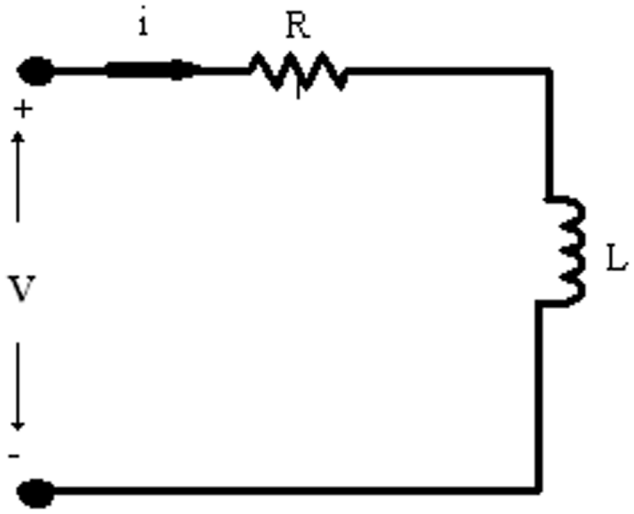

Figure 5: Equivalent circuit to calculate inductance

Figure 5. shows the equivalent circuit with zero state response to calculate inductance. The equivalent circuit consists of series resistance and inductance. Hence the time constant the series RL circuit is given by equation (2). from this time constant, inductance can be calculated as in equation (3). Equation (4) gives the total resistance of the equivalent circuit of SBSRM.

$$\tau = \frac{L}{R} \tag{2}$$

Where,

τ = is time constant.

$$L = \tau R \tag{3}$$

$$R = \frac{V}{I} \tag{4}$$

3.3. Torque

Torque is a very much important characteristic in SBSRM and is proportional to the torque winding current and is keep changing with respect to the rotor position. Hence inductance profiling has been done to determine the torque profiling. The amount of torque generated by SBSRM can be the slope of the torque winding. As the torque winding has high slope, this motor generates high torque. The effect of this generated torque is

very much less in SBSRM as the slope of the axial force winding is very less and also has negligible change in inductance with respect to the rotor position. Hence there is no mutual effect has been presented between torque and radial force, which indicates that both torque and radial force are completely decoupled from each other. Equation (5) shows the relation between torque, inductance and rotor position. Torque equation can also be represented as equation (6) by substituting inductance, it show the relation between torque and air gap length. Hence it is obvious that as decreasing the air gap length, high torque can be generated by this SBSRM.

$$T = \frac{1}{2} i^2 \frac{dL}{d\theta} \tag{5}$$

$$\mathrm{T} = \left(\frac{\mu_0 \mathrm{L\ r}\ (Ni)^2}{2\mathrm{g}} \right) \cdot \frac{\mathrm{d}\theta_a}{\mathrm{d}\theta} \tag{6}$$

3.4. Axial or Radial Force

The radial force is the special characteristic in SBSRM. This radial force can be increased and decreased with respect to the radial force winding current. The radial force can be controlled in both X and Y directions simultaneously by controlling the respective winding currents. Radial force is almost independent with the change in rotor position. As the motor rotates the, it will change in X-direction in a little, but there is no change in Y- direction with the same current. The radial force generated by the SBSRM has no effect on torque generated by the torque poles. Hence this SBSRM is very easy in controlling point of view

$$F = \frac{1}{2} i^2 \frac{dL}{dg} = \left(\frac{\mu_0 L\ r}{4} \right) \cdot \left(\frac{(Ni)}{g} \right)^2 \left(\theta_a + K_f \right) \tag{7}$$

Equation (7) shows the relation between axial force and air gap length. Large axial force can be generated by decreasing the air gap length.

4. SIMULATION RESULTS

Fig. 3 depicts the control schematic for the SBSRM. X* and Y* are the reference displacement signals, the values of reference displacement signals are zero; it means that rotor is being in center position. These reference displacement signals have been compared with the signals which are coming from two displacement sensors, one is placed in X-direction and another one is placed in Y direction. The error signals are given to the conventional PID controller. The output of the PID controllers are Fx* and Fy*, these are the command forces need to bring the rotor to center position. These command forces are given to the PWM logic block and generate eight PWM signals to the 4- phase asymmetric converter. This 4-phase converter suspends the rotor to the center position according the generated PWM signals. Now encoder giving the position information of the rotor, from this position speed is calculated using speed estimator block and this speed is compared with the speed command W* (reference speed). The error speed is given to the PI controller and generates command current im* and is given to the PWM block to generate four PWM signals to drive the 2-phase asymmetric converter. This 2-phase converter drives the rotor according to the generated PWM signals. Simulation results show the radial displacements in X-direction and Y-direction in micro meters, radial force winding currents in amps for four phases (IX+, IX-, IY+, IY-,), motor currents in amps for two phases (IA, IB), speed in rpm and torque in N. m. In the simulation, at a time two loads in both x- and y-direction of 10 N has been applied on shaft. Initial eccentric displacements in the both x & Y directions are -120 μm and -90 μm respectively. Figure.7

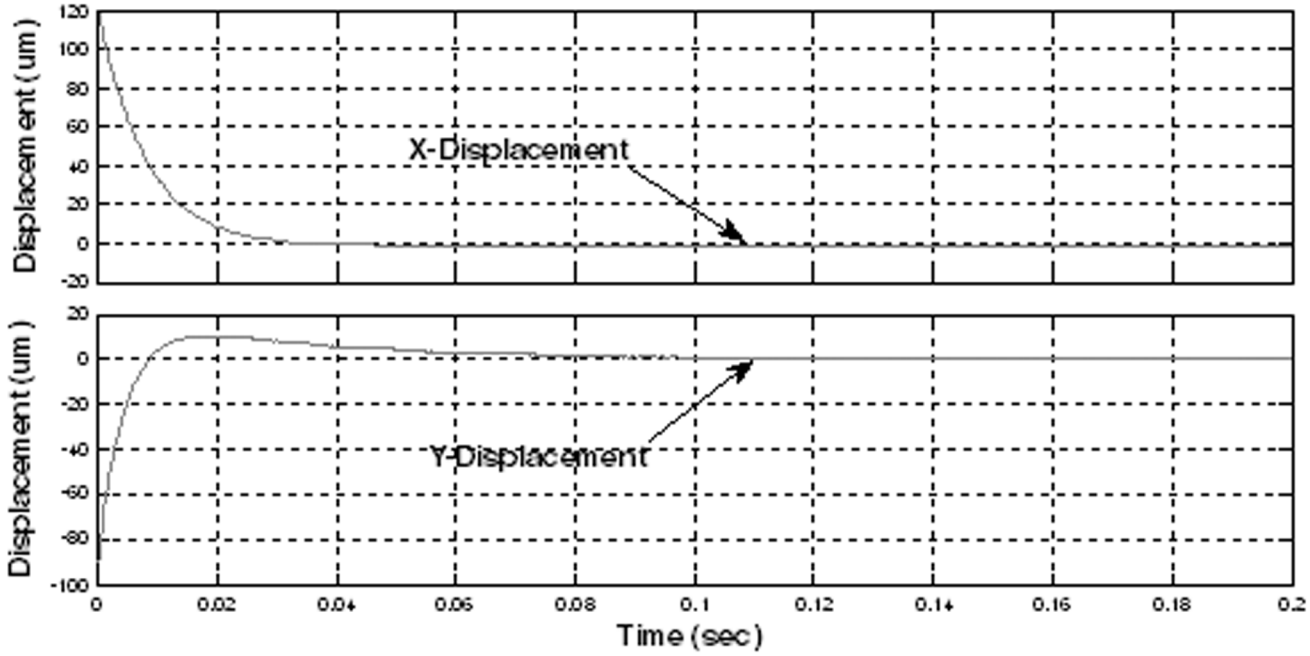

Figure 6: Displacements X and Y directions

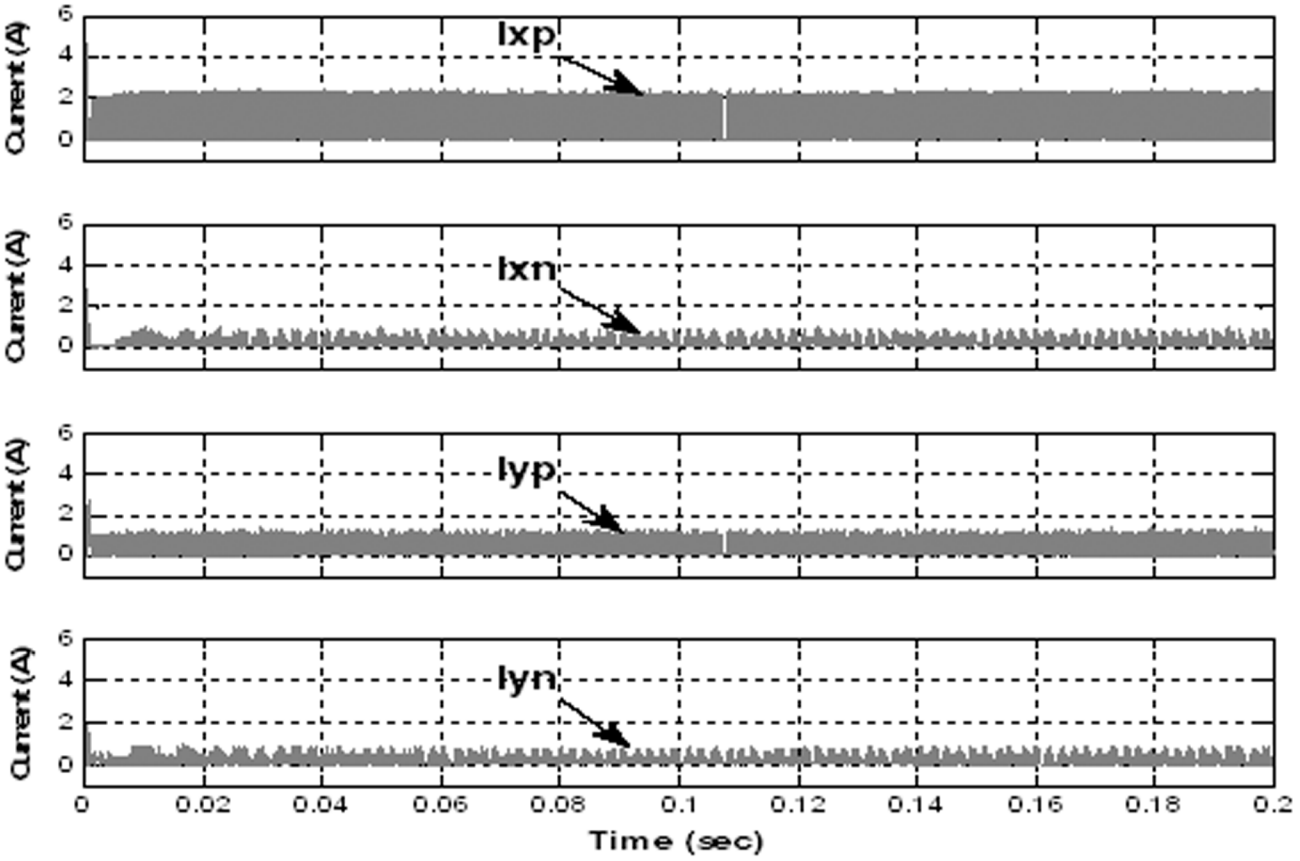

Figure 7: Axial force winding current

shows the rotor displacement movement in X- direction and Y directions respectively. Initially rotor is simulated at -120 and -90um in X&Y-direction respectively. By applying the effective controlling action with the conventional PID controller, these displacements have been settled at zero commands. Hence self bearing has been shown effectively with is simulation result.

Figure.7. shows the displacement currents of the four phase currents in positive and negative pole windings in both X and Y directions respectively. Where Ixp is the current in the positive X-directional pole winding, Ixn is the current in the negative X-directional pole winding; Iyp is the current in the positive Y-directional pole winding, Iyn is the current in the negative Y-directional pole winding. The nature of the suspension winding currents is DC currents, where as the nature of the torque pole winding currents are pulsating DC current signals. Initially suspension currents are high, after the rotor settled at center these currents are settled at 1A in average Figure.8. shows the torque winding currents of IA and IB. after the rotor settled at center position, load torque of 0.1 N. m has been applied on the shaft, as a results torque winding currents are injected to rotate the motor. As this motor has two phases (A-phase and B-phase) and as it is named as switched reluctance motor, at any instant only one phase is excited, which is shown in figure. 8. The nature of the torque winding currents is pulsating DC. At starting torque winding currents are drawn 4A, after speed reaches the commend speed torque winding currents are settled at nearly 1A. Figure.9. shows the speed and torque characteristics of the SBSRM. The speed has been settled at 0.05 seconds. And the torque produced by the motor is nearly 0.8 N.m at starting and is being settle at 0.2 N.m.

5. CONCLUSIONS

In this paper presents, the performance characteristics of self-bearing hybrid pole switched reluctance motor (SBSRM). This motor persist the advantages of the other type of bearingless motors and also carries the additional advantages like high torque short flux path, high power density, no flux reversal and high speed. Inductance profile of the radial force winding exhibits the independent characteristics with respect to the rotor position this shows the decoupling property of both torque winding and axial force characteristics. It generates very high torque at low input voltage. The simulation results shows characteristic of displacements and both X and Y direction and also shows how effectively rotor settled at center position. Suspension

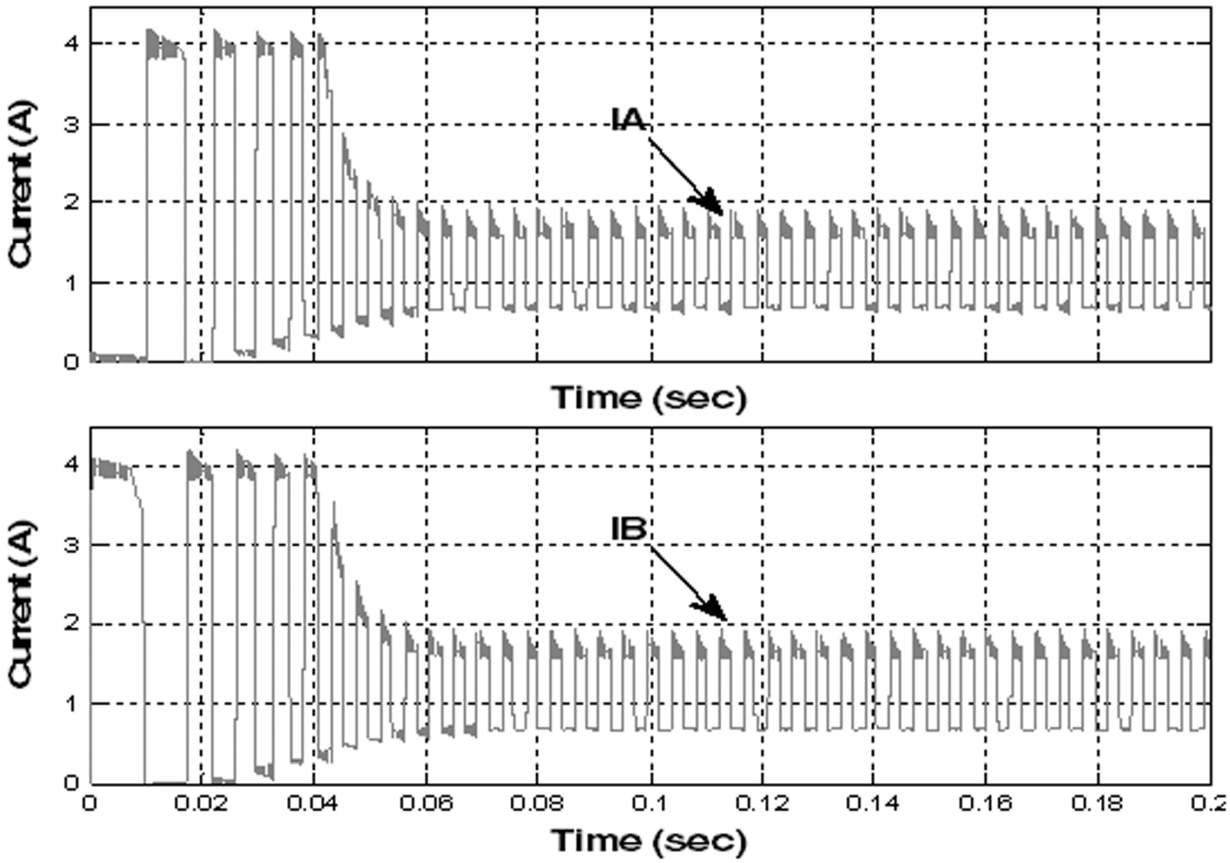

Figure 8: Torque winding currents

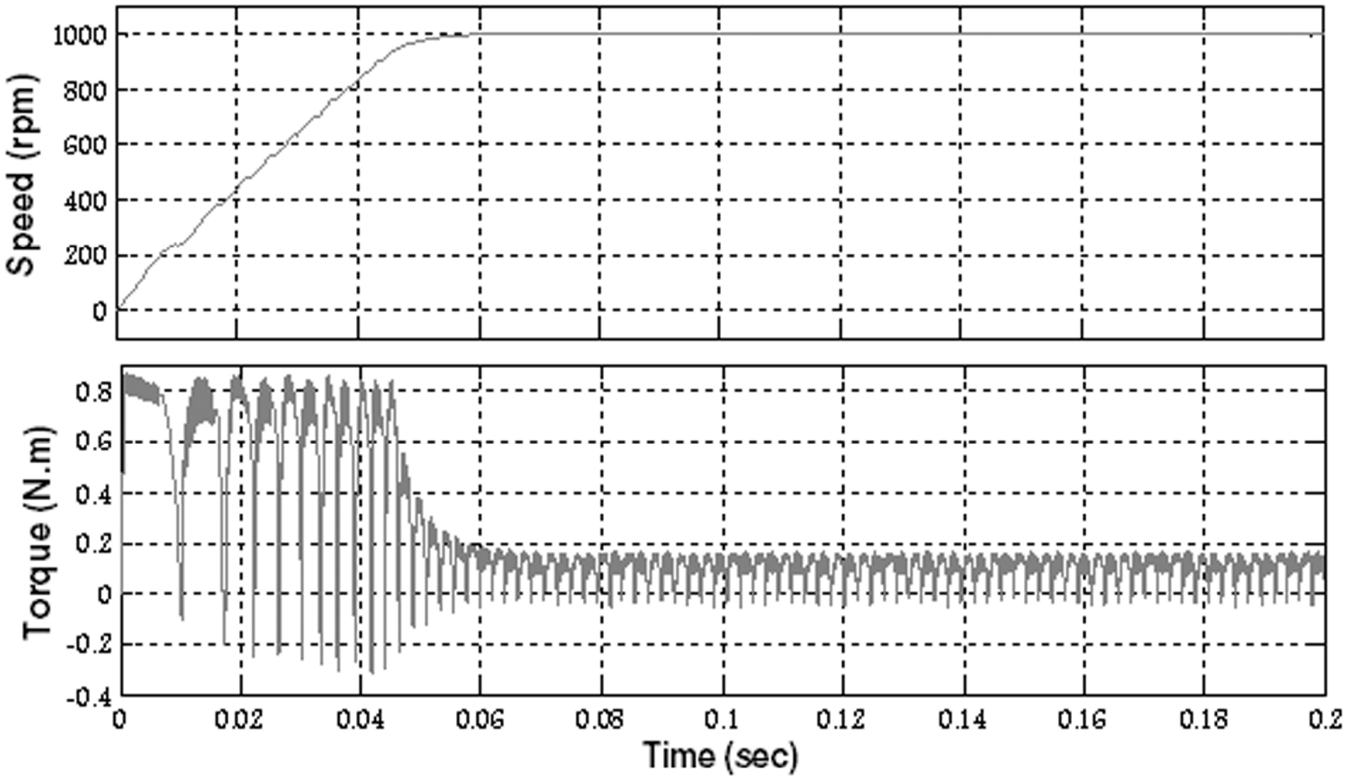

Figure 9: speed and torque

winding and torque winding currents are settled at lower values after steady suspension and after desired speed respectively. These types of motors are very much suitable in low power, high torque applications.

REFERENCES

[1] Dong-Hee Lee, Huijun Wang , Jin-Woo Ahn "Modeling and Control of Novel Bearingless Switched Reluctance Motor" in IEEE conference, 978-1-4244-2893:2009

[2] H. J. Wang, D. H. Lee and J. W. Ahn, "Novel Bearingless Switched Reluctance Motor with Hybrid Stator Poles: Concept, Analysis, Design and Experimental Verification," The Eleventh International Conference on Electrical Machines and Systems, 2008: 3358-3363.

[3] R. Bosch , "Development of a Bearingless Electric Motor," in Proc. Int. Conf. Electric Machines (ICEM'88), Pisa, Italy, 1988: 373-375.

[4] J. Bichsel, "The Bearingless Electrical Machine," in Proc. Int. Symp. Magn. Suspension. Technol, NASA Langley Res. Center, Hampton, 1991: 561-573.

[5] S. Ayari, M. besbes, M. Lecrivain, and M. Gabsi, "Effectes of the air gap eccentricity on the SRM vibrations," in Proc. Int. Conf. Electr. Mach. and Drives, 1999: 138-140.

[6] Dong-Hee Lee, Jin-Woo Ahn, "Design and Analysis of Hybrid Stator Bearingless SRM", Journal of Electrical Engineering & Technology, 2011, 6(1): 94-103.

[7] M. Takemoto, A. Chiba, H. Akagi and T. Fukao, "Radial Force and Torque of a Bearingless Switched Reluctance Motor Operating in a Region of Magnetic Saturation" in Conf. Record IEEE-IAS Annual Meeting, 2002: 35–42.

[8] Li Chen, Wilfried Hofmann, "Analytically Computing Winding Currents to Generate Torque and Levitation Force of a New Bearingless Switched Reluctance Motor", in Proc.12th EPE-PEMC, Aug, 2006: 1058-1063.

[9] M. Takemoto, A. Chiba, H. Akagi and T. Fukao, "Radial Force and Torque of a Bearingless Switched Reluctance Motor Operating in a Region of Magnetic Saturation" in Conf. Record IEEE-IAS Annual Meeting, 2002, pp. 35–42.

[10] M.Takemoto, A.Chiba, H.Suzuki, et al., "Radial Force and Torque of a Bearingless Switched Reluctance Motor Operating in a Region of Magnetic Saturation," IEEE Trans. on Industry Application, Jan./Feb. 2004, 40(1): 103-112.

[11] Li Chen, Wilfried Hofmann, "Analytically Computing Winding Currents to Generate Torque and Levitation Force of a New Bearingless Switched Reluctance Motor", in Proc.12th EPE-PEMC, Aug, 2006, pp. 1058-1063.